Birefringence imaging measurements on the phase diagram of $Pb(Mg_{1/3}Nb_{2/3})O_3$–$PbTiO_3$

2005 J. Phys.: Condens. Matter 17 1593

(http://iopscience.iop.org/0953-8984/17/10/014)

INSTITUTE OF PHYSICS PUBLISHING JOURNAL OF PHYSICS: CONDENSED MATTER

J. Phys.: Condens. Matter **17** (2005) 1593–1600 doi:10.1088/0953-8984/17/10/014

Birefringence imaging measurements on the phase diagram of $Pb(Mg_{1/3}Nb_{2/3})O_3$–$PbTiO_3$

D Zekria, V A Shuvaeva and A M Glazer

Physics Department, Oxford University, Parks Road, Oxford OX1 3PU, UK

Received 17 December 2004, in final form 17 December 2004
Published 25 February 2005
Online at stacks.iop.org/JPhysCM/17/1593

Abstract

The phase diagram of $(PbMg_{1/3}Nb_{2/3}O_3)_{1-x}$–$(PbTiO_3)_x$ (PMN–PT) has been determined to high accuracy over the whole compositional range using birefringence imaging. A steep change has been detected in the thermal hysteresis of phase transitions in the morphotropic phase boundary region at $x = 0.295$ at the boundary between relaxor and non-relaxor phases. At the same composition at a temperature about 30 °C below T_c a monoclinic phase appears. The phase transition between non-relaxor and the monoclinic phase is characterized by a pronounced thermal hysteresis and a large jump in birefringence, showing that this is of first order. A significant change in slope for the compositional dependence of T_c has been found for $x \simeq 0.45$, suggesting a boundary between the tetragonal phase and a phase of lower symmetry. The temperature dependence of the birefringence has been measured for a number of different compositions in the range $0.3 < x < 1$, in which it is found that the birefringence of the monoclinic phase is much higher than that seen in the other phases for $x < 0.5$.

1. Introduction

The morphotropic phase boundary (MPB) in PMN–PT and analogous materials has attracted much attention because it is in this region of the phase diagram that the materials exhibit a large increase in piezoelectric activity [1–5]. It was originally believed that the MPB occurs between two phases, one of rhombohedral symmetry and the other of tetragonal symmetry. The transformation from rhombohedral to tetragonal symmetry, given that the two phases are not group–subgroup related, has been the subject of much discussion. Several attempts at constructing the composition–temperature phase diagram of PMN–PT have been made, starting from the work of Ouchi *et al* [6], who plotted Curie temperature against composition for a range of PMN–PT ceramics. This plot, though somewhat crude, showed a vertical line at a composition of approximately $x = 0.4$ separating the pseudocubic phase associated with lead magnesium niobate (PMN) from the tetragonal phase characteristic of lead titanate (PT).

Subsequent efforts to map out the phase diagram have focused on the MPB region, but nevertheless, much uncertainty persists. Kelly *et al* [7] observed the MPB composition to lie at $x = 0.345$, with a region of coexistent rhombohedral and tetragonal phases spanning $x = 0.28$–0.40. Choi *et al* [8] found that the MPB lies in the range $x \sim 0.30$–0.325. Shrout *et al* [9] showed an MPB extending over about $x \sim 0.26$–0.34 in their phase diagram, whilst Noblanc *et al* [10] claimed that a mixed rhombohedral–tetragonal phase region exists over about $x = 0.28$–0.41 at room temperature. Noheda *et al* [11], on the other hand, found a monoclinic phase over about $x = 0.30$–0.38, which is consistent with Singh and Pandey's [12] claim that the composition at $x = 0.34$ is monoclinic with space group Pm, though in a later publication [13], the same authors reported two monoclinic phases, one of space group Cm in the range $0.27 \leqslant x \leqslant 0.30$, and the other of Pm symmetry in the range $0.31 \leqslant x \leqslant 0.34$.

It should be pointed out that the above reports were all based on measurements of ceramic and powder samples, and this could account for some of the inconsistencies between the various reports. Apart from the inherent composition distribution on the nanoscale, believed to be the underlying cause of relaxor properties, ceramics are more likely to suffer from macroscale inhomogeneities dependent on the method of synthesis. Any spread in the actual composition will increase the imprecision associated with locating a phase transition, not to mention reducing the certainty of the absolute value of the composition.

Optical microscopy is one of the most effective and accurate tools for the determination of phase transition points and for constructing phase diagrams from crystalline samples. Numerous optical studies of PMN–PT crystals have been reported recently [14–18]; however only in one of them [17] has this method been employed for mapping out the boundaries of the intermediate phase. In particular, in this work the method of birefringence imaging using a Metripol microscope (www.metripol.com) was applied to study a single crystal with a composition gradient spanning the MPB composition, which allowed data on the phases to be obtained with unprecedented precision and resolution from a single sample and the phase diagram of PMN–PT to be built in a narrow compositional range around the MPB.

In the present research, we have employed the same birefringence imaging technique on a series of PMN–PT single-crystal samples with compositions across the solid-solution spectrum, and report a more extended view of the phase diagram around the MPB. In addition, the absolute birefringence of a number of the compositions in the range $0.3 < x < 1$ have been determined.

2. Experimental details

2.1. Sample preparation

Single crystals of differing composition were prepared from MgO, Nb_2O_5, TiO_2 and PbO, with a 300% excess of the latter to serve as a flux. Powders of the starting materials were ground together in appropriate proportions, and then transferred to 25 ml platinum crucibles, onto which loose-fitting lids were placed. The mixtures were heated to 1393 K at a rate of 50 K h^{-1}, held at this temperature for 24 h, and then cooled at 1 K h^{-1} to 1143 K. They were subsequently cooled at 100 K h^{-1} down to room temperature. The crystals were separated from the remaining flux by soaking in hot concentrated nitric acid.

It is believed that evaporation of the lead oxide, and consequent saturation of the solution, plays a key role in the crystallization process of this method. However, as the rate of evaporation is difficult to control in our set-up, the crystal quality tended to show some inconsistencies. In all cases, the actual titanium content of the crystals was lower than the proportion in the starting mixture, ranging up to a deficiency of about 10%.

The crystals were polished to thin sections of approximately 50 μm. Crystals with well-formed natural $(100)_p$[1] faces were selected because they served as convenient reference planes for polishing the crystal sections in corresponding orientations. Apart from the titanium deficiency referred to above, it was found that the crystals were not uniformly homogeneous, with some showing a significant composition gradient within a single sample.

2.2. *Compositional analysis*

The local compositions at different positions of the samples were determined by electron-probe microanalysis (EPMA) (Jeol JXA-8600). Corresponding locations were studied with EPMA and optically, so that the correct association between composition and phase transition temperature could be made even when the crystal was inhomogeneous. A spot size of about 10 μm was used, so that compositional fluctuations on smaller scales would not be resolved. The composition of one of the crystals employed in the study gradually changed from $x = 0.29$ to 0.37 across the crystal which enabled us to carefully map out the phase transition temperatures in the MPB region in small compositional steps.

2.3. *Metripol optical measurements*

The crystals were studied using a Metripol microscope. Briefly, this is a microscope system equipped with a plane polarizer capable of being rotated to fixed angles α from a reference position, a circular analyser and a CCD camera [19]. The transmitted intensity measured at any position within the captured image is given by the formula

$$I = \frac{I_0}{2}[1 + \sin(2\phi - 2\alpha)\sin\delta] \tag{1}$$

in which I_0 is the intensity of the light through the sample, representing its transmittance. ϕ is the angle of the slow axis of the optical indicatrix of the specimen with respect to the reference position (ϕ corresponds to the angle of optical extinction) and δ is the phase shift of the polarized light components, expressed by

$$\delta = \frac{2\pi}{\lambda}(n_1 - n_2)\tau = R\tau. \tag{2}$$

λ is the wavelength of the light, τ is the thickness of the sample and $(n_1 - n_2)$ is the so-called planobirefringence. R, the retardance, is a measure of the birefringent power of a particular thickness of the material. The advantage of this imaging system is that by acquiring several images with varying angle α, the orientation ϕ and the retardance-related $|\sin\delta|$ can be determined separately for any point of the imaged sample. New images are then computed in which each quantity is plotted in false colours. The resulting images are not only qualitative, but also quantitative, since actual values can be read off at any point in the image.

The microscope was equipped with a Linkam (THMSG600) microscope heating stage, and so the temperature dependence of the birefringence could then be extracted from the $|\sin\delta|$ data. However, note that, as $|\sin\delta|$ is a periodic function, we cannot in general judge from its value alone the absolute value of δ, and consequently the birefringence. Thus, an independent method for determining the absolute value is required at at least one temperature, which can then serve as a reference on which the other values are based.

In our experiments the temperature was raised from 83 K to that of the highest-temperature phase, at a rate of 1 K min^{-1}. By collecting a data set every 30 s whilst heating, the retardance of the sample could be tracked with respect to temperature. Whenever a phase transition

[1] The subscript p denotes pseudocubic perovskite axes.

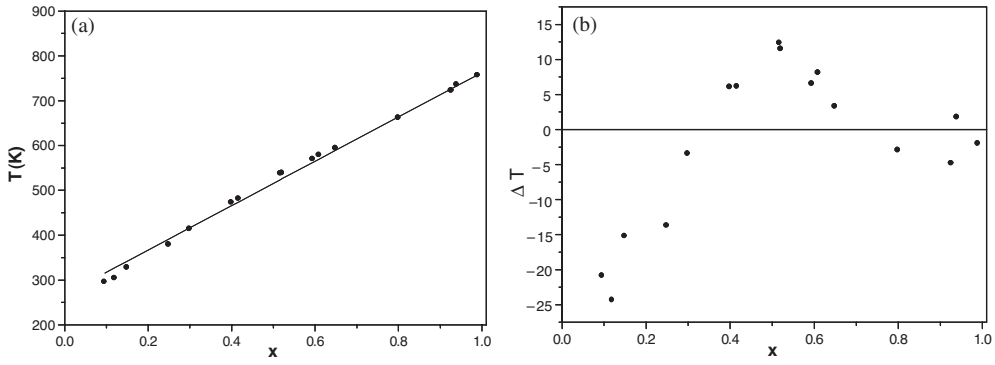

Figure 1. (a) The compositional dependence of T_c and (b) the difference from a straight-line fit.

occurred, the retardance was seen to undergo an abrupt change. Observation of the retardance therefore provides a sensitive method by which the temperatures of the phase transitions of a particular sample can be determined. Similar experiments were conducted whilst cooling the crystals.

3. Results and discussion

3.1. Compositional dependence of T_c

The composition at each measured point was accurately correlated with its corresponding phase transition temperature to the cubic phase, at which total extinction was achieved. As a result the compositional dependence of T_c was obtained (figure 1).

On the assumption that T_c depends linearly on composition we obtained the following expression based on T_c for pure $PbTiO_3$ and pure PMN equal to 763 and 268 K, respectively:

$$T_c = 268 + 494x. \tag{3}$$

This line together with the experimental points is shown in figure 1(a), while in figure 1(b) the difference between experimental and calculated T_c is plotted. It can be seen that this difference can be as large as 25 K and the shape of the curve suggests that the experimental points can be fitted much more accurately if the linear fits are made separately for $x < 0.5$ and $x > 0.5$. The results of such fits are shown in figure 2 and as a result the experimental $T_c(x)$ dependence is represented by two straight lines with slightly different slopes expressed by the formulae

$$T_c = 236 + 586x \qquad \text{for } x < 0.5 \tag{4}$$

and

$$T_c = 293 + 465x \qquad \text{for } x > 0.5. \tag{5}$$

These lines intersect at $x \simeq 0.45$, i.e. rather far from the MPB region. Previous experiments on the region around $x = 0.3$ have shown that the change of slope in $T_c(x)$ at the MPB is very slight [1, 8, 20, 21]. This is supported by our results which show that the whole region with $x < 0.5$ can be fitted to rather high precision with a single straight line. The significant change in slope close to $x = 0.45$ may be associated with some structural change occurring at this point, and suggests the need to take a close look at this particular region.

Comparison of T_c measured on heating and on cooling in samples with composition varying across the MPB showed that significant thermal hysteresis occurred in samples with

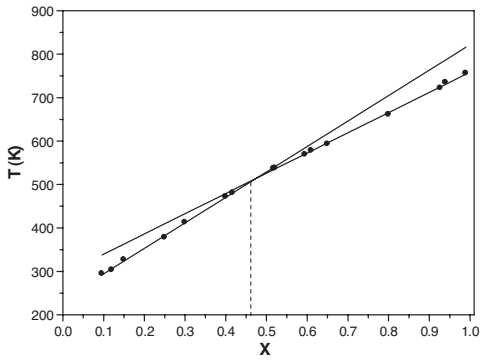

Figure 2. The compositional dependence of T_c fitted with two straight lines separately for $x > 0.5$ and $x < 0.5$.

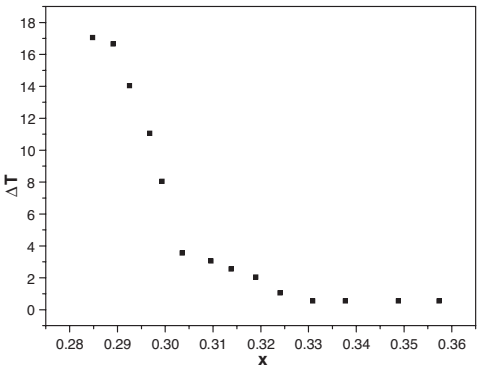

Figure 3. The compositional dependence of the thermal hysteresis of the transition to the cubic phase in the MPB region.

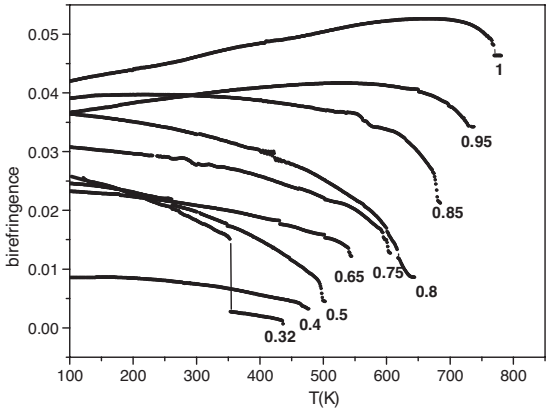

Figure 4. The temperature dependence of the birefringence of PMN–PT crystals.

low titanium content ($x < 0.3$) while in the Ti-rich crystals it was negligible. The thermal hysteresis in the MPB region is plotted as a function of composition in figure 3.

It can be seen that it changes abruptly at $x = 0.295$, which corresponds to the point where dielectric frequency dispersion abruptly appears [20, 22, 23]. The thermal hysteresis thus obtained has a similar dependence on composition to the difference of transition temperatures determined via dielectric measurements at 100 Hz and 100 kHz [8], showing that this composition marks the change from relaxor to non-relaxor ferroelectric behaviour.

3.2. Temperature and compositional dependence of birefringence

The temperature dependence of birefringence of $PbTiO_3$ has been intensively studied over several decades [24–29], and is known to have a maximum just below the phase transition into the cubic phase. The birefringence in a number of tetragonal PMN–PT crystals with $x > 0.3$ (figure 4) shows that the characteristic shape of the curve for pure PT quickly disappears with the addition of PMN into the structure. The peak is still observed in crystals of composition $x = 0.95$ and 0.85, albeit at a reduced temperature, though compositions richer in PMN display the more typical negative birefringence–temperature slope over the entire temperature range measured.

The absolute magnitude of the birefringence decreases with decreasing PT content. This result is similar to the measurements of Fushimi and Ikeda [29] on the analogous system lead zirconate–titanate ($PbZr_xTi_{1-x}O_3$), which also showed that the birefringence decreased as the composition tended away from the titanium-rich end of the range. For $x < 0.3$ the room temperature birefringence is very low and inhomogeneous, so that in some parts of the crystal it even attains a value close to zero. For $x = 0.30$–0.37 it increases considerably, dropping suddenly around $x = 0.37$ to a minimum at $x = 0.4$. Among all the phases of PMN–PT which exist in the compositional range $x < 0.5$, only the one which, according to x-ray diffraction studies [11–13], corresponds to the monoclinic region has a high birefringence, and so its boundaries can be clearly observed.

The birefringence results in the MPB region are in generally good agreement with that reported by Ye and Dong [30], showing a very similar compositional and temperature dependence, although in terms of absolute values, some discrepancy exists between our results and theirs. These inconsistencies can be explained by the high sensitivity of the birefringence to any crystal imperfection and the need for very accurate determination of sample thickness. The compositional dependence of birefringence also shows much similarity with the compositional behaviour of the spontaneous polarization reported by Choi [8].

3.3. The morphotropic phase boundary region ($x = 0.28$–0.38)

The observed smooth one-dimensional compositional gradient in our samples has enabled us to observe clearly all the steps in a complicated series of phase transformations simultaneously as a function of composition and time. Within the compositional range $0.28 < x < 0.38$ three different phases were clearly observed through the contrast in their birefringence and difference of optical extinction angle. As we have shown already, the jump in T_c hysteresis indicates that the composition $x = 0.295$ denotes a boundary between two different phases corresponding to relaxor and non-relaxor states, phases I and II, respectively. This boundary can also be seen at lower temperatures through the differences in optical extinction angle, birefringence value and domain structure within the temperature range 383–410 K. At exactly the same composition a highly birefringent phase, corresponding to the monoclinic phase (II), emerges at a temperature about 30 K below T_c.

Figure 5 shows three $|\sin\delta|$ images of a crystal with changing composition taken at three different temperatures. At 404 K a sharp vertical boundary is seen separating the cubic phase on the left and phase I, with another boundary between I and III (see figure 6). At 383 K the vertical boundary now separates the relaxor phase I on the left and the non-relaxor phase III on the right, without passing through the monoclinic phase II. At 378 K we observe the boundary between the relaxor phase I on the left and the monoclinic phase II on the right.

The symmetries of all these phases are still a matter of debate and controversy persists in numerous recent papers devoted to the subject [11, 13, 14, 16]. This question will be addressed in detail at a later date, but for the present we show in figure 6 an accurate map of the points at which jumps of birefringence were recorded. Phase I is often referred to as a rhombohedral relaxor phase, although there is evidence that in fact it may be monoclinic [13]. Phase II corresponds to the monoclinic region reported by Noheda *et al* [11] and by Singh and Pandey [12, 13]. Phase III has hitherto been considered to be a non-relaxor tetragonal phase; however Zekria *et al* [17] and Tu *et al* [16] found that in this region the optical extinction angle showed a variation with composition and temperature. When taken with our evidence of a transition possibly occurring at $x \simeq 0.45$ this suggests that in fact this region is a distinct phase of lower symmetry than tetragonal with the true tetragonal phase appearing for $x > 0.45$.

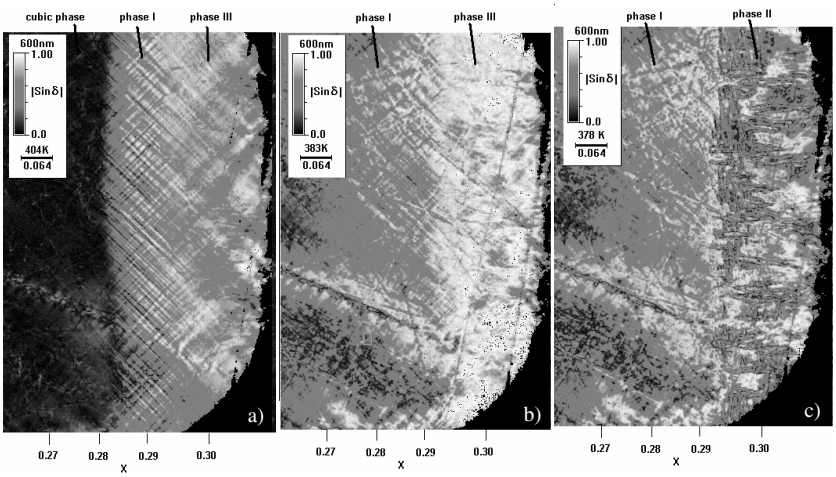

Figure 5. Metripol $|\sin\delta|$ images of a PMN–PT crystal with a compositional gradient in the horizontal direction: (a) $T = 404$ K on heating, paraelectric cubic phase on the left, phase I in the middle and phase III on the right; (b) $T = 383$ K on cooling, phase I on the left and phase II on the right; (c) $T = 378$ K on cooling, phase I on the left and phase II on the right.

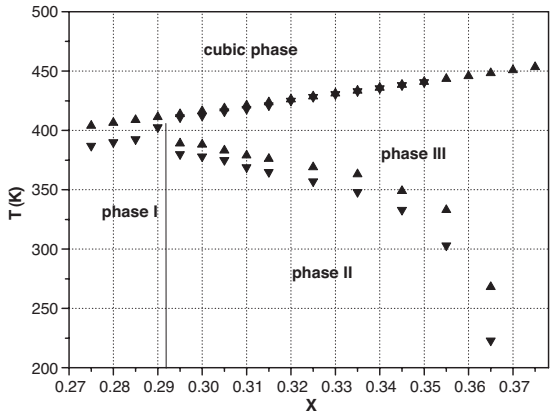

Figure 6. The phase diagram of PMN–PT in the morphotropic region measured on heating, ▲, and cooling, ▼.

Interestingly, Glazer *et al* [31] suggested the possibility of another monoclinic phase at the MPB also in the perovskite $PbZr_xTi_{1-x}O_3$.

The temperature–composition phase diagram of PMN–PT (figure 6) is in general agreement with the previously published diagrams. In particular, it is in good correspondence with that of Noheda [11] which was based on diffraction measurements on ceramic samples, although the one presented here is much more accurate and detailed. The phase transition points in the phase diagram were measured both on heating and on cooling and thus a large thermal hysteresis between phase II and the non-relaxor phase III has been observed. Along with the large jump of birefringence this shows that this transition is of first order.

4. Conclusions

As a result of the optical studies of PMN–PT crystals we have obtained accurate values for the phase transition temperatures on heating and on cooling and have mapped the boundaries of

the phases in the MPB region. From the results obtained we can conclude that:

(1) The slope of T_c as a function of x changes at about $x = 0.45$, probably indicating a phase boundary between the tetragonal phase and a hitherto unreported phase of lower symmetry.
(2) Relaxor–cubic and monoclinic–non-relaxor phase transitions show a large thermal hysteresis, while in the non-relaxor–cubic phase transition it is close to zero.
(3) The monoclinic phase II does not completely separate relaxor I and non-relaxor III phases, which have a common boundary in the temperature range 393–413 K.
(4) The monoclinic phase II has a much higher birefringence compared with that in the other phases in the compositional range $x < 0.5$.

Acknowledgments

We are grateful to the Engineering & Physical Sciences Research Council (UK) for grants enabling this work to be carried out.

References

[1] Choi S W, Shrout T R, Jang S J and Bhalla A S 1989 *Ferroelectrics* **100** 29
[2] Shrout T R, Chang Z P, Kim N and Markgraf S 1990 *Ferroelectr. Lett.* **12** 63
[3] Service R E 1997 *Science* **275** 1878
[4] Fu H and Cohen R E 2000 *Nature* **403** 281
[5] Zhao X, Fang B, Cao H, Guo Y and Luo H 2002 *Mater. Sci. Eng.* B **96** 254–62
[6] Oguchi H, Nagano K and Hayakawa Sh 1965 *J. Am. Ceram. Soc.* **48** 630–5
[7] Kelly J, Leonard M, Tantigate C and Safari A 1997 *J. Am. Ceram. Soc.* **80** 957–64
[8] Choi S W, Jung J M and Bhalla A S 1996 *Ferroelectrics* **189** 27–38
[9] Shrout T R, Chang Z P, Kim N and Markgraf S 1990 *Ferroelectr. Lett.* **12** 63–9
[10] Noblanc O, Gaucher P and Calvarin G 1996 *J. Appl. Phys.* **79** 4291–7
[11] Noheda B, Cox D E, Shirane G, Gao J and Ye Z-G 2002 *Phys. Rev.* B **66** 054104
[12] Singh A K and Pandey D 2001 *J. Phys.: Condens. Matter* **13** L931–6
[13] Singh A K and Pandey D 2003 *Phys. Rev.* B **67** 064102
[14] Xu G, Luo H, Xu H and Yin Z 2001 *Phys. Rev.* B **64** 020102
[15] Ye Z-G and Dong M 2000 *J. Appl. Phys.* **87** 2312–9
[16] Tu C-S, Schmidt V H, Shih I-C and Chien R 2003 *Phys. Rev.* B **67** 020102
[17] Zekria D and Glazer A M 2004 *J. Appl. Crystallogr.* **37** 143–9
[18] Bokov A A and Ye Z G 2004 *J. Appl. Phys.* **95** 6347–59
[19] Glazer A M, Lewis J G and Kaminsky W 1996 *Proc. R. Soc.* A **452** 2751–65
[20] Han J and Cao W 2003 *Phys. Rev.* B **68** 134102
[21] Colla E, Yushin N and Viehland D 1998 *J. Appl. Phys.* **83** 3298–304
[22] Feng Z, Zhao X and Luo H 2004 *J. Phys.: Condens. Matter* **16** 6771–8
[23] Ohwa H, Iwata M, Orihara H, Yasuda N and Ishibashi Y 2001 *J. Phys. Soc. Japan* **70** 3149–54
[24] Kleeman W, Schaefer F J and Rytz D 1986 *Phys. Rev.* B **34** 7873–9
[25] Kobayashi J 1958 *J. Appl. Phys.* **28** 866–7
[26] Fesenko E G and Kolesova R V 1959 *Kristallographiya* **4** 60–4
[27] Mabud S A and Glazer A M 1979 *J. Appl. Crystallogr.* **12** 49–53
[28] Zekria D, Glazer A M, Shuvaeva V, Dec J and Miga S 2004 *J. Appl. Crystallogr.* **37** 551–4
[29] Fushimi Sh and Ikeda T 1965 *J. Phys. Soc. Japan* **20** 2007–12
[30] Ye Z-G and Dong M 2000 *J. Appl. Phys.* **87** 2312–9
[31] Glazer A M, Thomas P A, Baba-Kishi K Z, Pang G K H and Tai C W 2004 *Phys. Rev.* B **70** 184123